J Therm Anal Calorim (2012) 110:37–41
DOI 10.1007/s10973-011-1880-3

Dehydration investigations of a refractory concrete using DTA method

N. Obradović · A. Terzić · Lj. Pavlović · S. Filipović · V. Pavlović

CEEC-TAC1 Conference Special Chapter

Abstract The base mix refractory concrete is corundum-based, containing corundum as refractory aggregate and CAC as hydraulic binder, with a spinel as an additive. The authors investigated the dehydration reactions which occur from the moment when water is added (at the beginning of components mixing), to the moment when installed refractory concrete lining is put into the service. Sintering process kinetic of low-cement content refractory concrete was investigated by means of differential thermal analysis at four different heating rates (5, 10, 20, and 30 °C/min). Thus, temperature was increased from 20 to 1100 °C. It was noticed that first dehydration step occurs at lower temperatures, indicating at a desorption of physically adsorbed and interlayer water molecules. Second dehydration step, at higher temperatures is due to dehydroxylation of the lattices and decomposition of the interlayer anions.

Keywords Sintering kinetics · DTA · Refractory concrete

Introduction

Monolithic refractory concretes with calcium aluminates cement as binding agent have been manufactured for over 80 years now. First, refractory concretes were based on high cement formulations. Today, accent is on reducing cement content in concrete systems. Such concretes can be placed as shotcrete, gunning, self-flowing, or pumping. Calcium aluminates cements (CAC), in both cases, play major role in determining the properties on refractory concretes [1].

Several steps precede the usage of CAC based monolithic refractory concretes: (1) mixing, (2) placing and consolidation, (3) storage, (4) drying and, subsequently, (5) final use in service. Each step in concrete placing is closely linked to the hydration process of CAC.

Thus, it is necessary to consider the reaction that take place within CAC during the hydration process in order to understand the role of CAC in refractory concrete. The cementitious (bonding) properties enable the refractory concrete to be cast in place and to set and harden at ambient temperature. During the heating phase of refractory concrete water, which is necessary for hydration products formation, is driven off. In such condition, hot compressive strength is provided by sintering and ceramic bonding [2].

This article is concerned with investigation of dehydration reactions which occur from the moment when water is added (at the beginning of components mixing), to the moment when installed refractory concrete lining is put into the service. Investigation described in this article points out to the effect of dehydration reactions on properties of refractory concrete and the impact of temperature and mineralogy on behaviour of concrete lining [3].

Experimental procedure

Materials

Experiments were performed using one composition of refractory concrete. The base mix refractory concrete is

N. Obradović (✉) · S. Filipović · V. Pavlović
Institute of Technical Sciences-SASA, Knez Mihajlova 35/IV, 11000 Belgrade, Serbia
e-mail: nina.obradovic@itn.sanu.ac.rs

A. Terzić · Lj. Pavlović
Institute for Technology of Nuclear and Other Raw Materials, F. d′Eperey 86, 11000 Belgrade, Serbia

corundum based, containing corundum as refractory aggregate (75 wt%; particle size: 0–1, 1–3, 3–5 mm) and CAC as hydraulic binder (15 wt%). A spinel, $MgO{\cdot}Al_2O_3$, was used as an additive in concrete mixture. A chemical composition of starting raw materials obtained by atomic absorption spectrophotometer, AAS Analyst 300, is given in Table 1.

Samples preparation procedure and investigation methods

The concrete mixture was prepared and cured according to Standard SRPS B.D8.300. Designed concrete samples contained corundum as the refractory aggregate and CAC as a bonding agent. A spinel was used as an additive in concrete mixtures.

Concrete mixture was mixed for 8 min in a laboratory RILEM-cem mixer. Afterwards, mixture was poured into moulds and cured for 24 h at room temperature (20 °C) in a controlled relative humidity ($\varphi = 60\%$). After 24 h, the samples gained enough mechanical strength so they could be removed from the moulds. After removal from the moulds, samples were returned to the controlled humidity environment (20 °C and relative humidity $\varphi = 60\%$) for 7 days, than they were dried at 110 °C for 24 h.

Concrete specimens were tested for compressive strength (CS—sample dimensions: 100 × 100 × 100 mm) and flexural strength (FS—sample dimensions: 40 × 40 × 160 mm) using a laboratory hydraulic press (Standard: SRPS U.M1.005 and SRPS U.M1.020, number of samples was 6). Pressure was applied vertically using axial force on one side of a cubic sample, in CS testing. In FS testing, pressure was applied vertically, on two-thirds of the length of longest side of prismatic sample.

Apparent porosity (P) was investigated using a mercury porosimeter on 100 × 100 × 100 mm samples.

Refractoriness under load was tested on 50 mm high by 50 mm diameter cylindrical samples using a 0.2 MPa load. Refractoriness under load was tested at room temperature. Time used for the test was 72 h. Refractoriness was investigated on pyramid-shaped samples (10 × 10 × 45 mm) in standard Netzsch furnace PCE 428 for refractoriness testing. Temperature increasing rate was 4 °C/min.

X-ray powder diffraction pattern of concrete sample was obtained using a Philips PW-1050 diffractometer with λCu-K_α radiation and a step/time scan mode of 0.05°/1 s.

The morphology of concrete was characterized by scanning electron microscopy (JEOL JSM-6390 LV). The sample was crushed and covered with gold in order to perform these measurements.

The DTA was performed with a SHIMADZU DTA-50 apparatus. About 30 mg sample was used for DTA testing and α-Al_2O_3 powder as the reference sample. The heating temperature range was from room temperature to 1,100 °C at heating rates of 5, 10, 20, and 30 °C/min. The measurement was carried out in nitrogen flow at the rate of 20 mL/min.

Results and discussion

Chemical analysis

A chemical composition of the designed concrete mixtures, obtained by atomic absorption spectrophotometer, AAS Analyst 300, is given in Table 2.

High level of MgO content in refractory concrete originates from synthetic spinel, $MgO{\cdot}Al_2O_3$.

Minerological analysis

Minerological analysis of green refractory concrete was performed by means of XRD method. Results of analysis are presented in Table 3 and Fig. 1.

By means of XRD method, the following phases were found: α-Al_2O_3 corundum, $Al(OH)_3$ gibbsite, spinel phase, $Ca_{12}Al_7H_8$, and CA originate from cement.

Table 1 Chemical analysis of starting raw materials

Content/%	Al_2O_3	SiO_2	CaO	MgO	Fe_2O_3	Na_2O	K_2O	TiO_2	L.O.I.
Raw material									
CAC	68.9	0.1	29.7	0.1	0.1	0.3	–	–	0.6
Corundum	99.8	0.1	–	–	0.1	0.2	–	–	–
Spinel synth.	59.1	2.4	0.4	35.2	2.9	–	–	0.3	0.8

Table 2 Chemical analysis of corundum-based refractory concrete

Content/%	Al_2O_3	SiO_2	CaO	MgO	Fe_2O_3	Na_2O	TiO_2	L.O.I.
Concrete mixture	86.8	0.4	1.4	5.4	0.1	0.9	–	5.8
Fired concrete	92.0	0.4	1.5	5.7	0.1	0.9	0.3	–

Table 3 XRD analysis of refractory concrete mixture

Mineral phases	α-Al_2O_3 corundum	$Al(OH)_3$ gibbsite	Spinel phase	$C_{12}Al_7H_8$	CA
Phasecontent	+++	+++	++	+	+

+ low, ++ medium, +++ high quantity

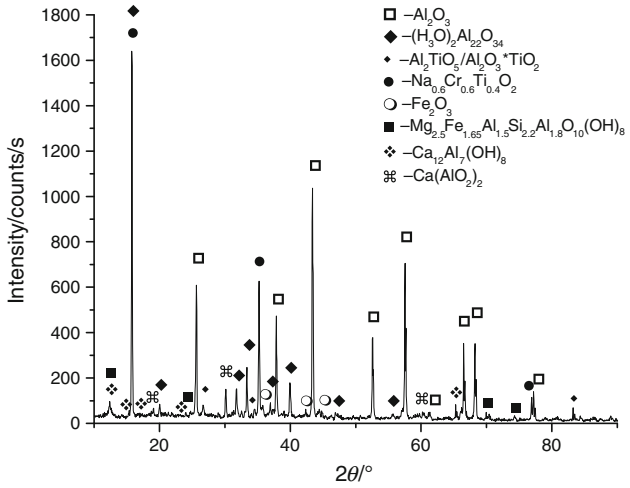

Fig. 1 XRD pattern of concrete sample

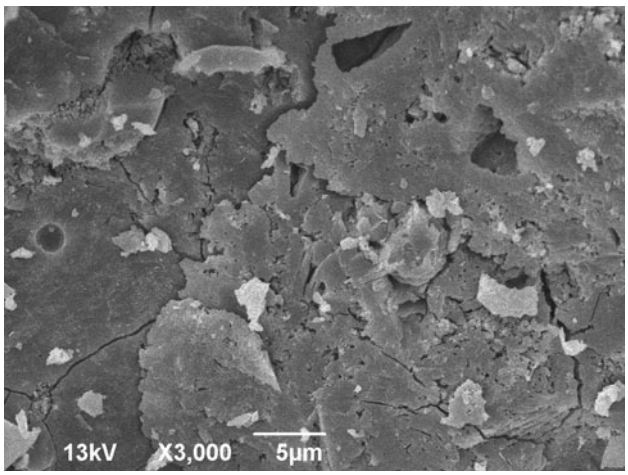

Fig. 2 SEM micrograph of concrete sample

Microstructural analysis

Figure 2 shows SEM micrograph of concrete sample. As it is well known concrete is a complex, heterogeneous multiphase material, which is often considered to be a three-phase composite structure. Its structure includes aggregate particles, the cement paste matrix in which they are dispersed, and the interfacial transition zone around the aggregate particles and cement paste. Concrete often exhibits random microstructure at different length scales ranging from the nanometres scale to the macroscopic decimetres scale. According to our microstructure analysis aggregate particles, several millimetres in size are surrounded with a fine matrix composed of micron sized particles. Cement paste and fine, coarse aggregates, with a range of sizes and shapes as well as crack structures and pores of various sizes were also noticed. It should be noticed that the structure of the porosity in concrete strongly influences its properties. Their structure is related to the original packing of the cement, mineral admixtures, and the aggregate particles, to the water-to-solids ratio, etc. [4].

According to Brown et al. [5], sources of porosity in concrete include: gel pores, smaller capillary pores, larger capillary pores, large voids, porosity associated with paste-aggregate interfacial zones, micro cracks, and porosity in aggregate. Although, it is considered that because gel porosity resides in the hydration products that accumulate between the liquid phase and the anhydrous cement grains, gel porosity has a major effect on hydration rates, the contributions of each of the remaining types of porosity should not be neglected either.

Table 4 Physico-mechanical properties of refractory concrete

Temperature/°C	Porosity/%	Compressive strength/MPa	Water absorption/%	Bulk density/g/cm^3
20	2.8	78.9	0.9	3.1

Table 5 Refractoriness under load and refractoriness

T_a/°C	T_e/°C	SK/temperature/°C
1,450	>1,600	34/1755

Physico-mechanical properties of refractory concrete

Investigated physico-mechanical properties (porosity, compressive strength, water absorption, bulk density, refractoriness under load, and refractoriness) of refractory concrete are presented in Tables 4 and 5.

Investigated concrete samples showed extremely high comprehensive strength, and equally low level of porosity. Thus, values of refractoriness and refractoriness under load are high, as expected.

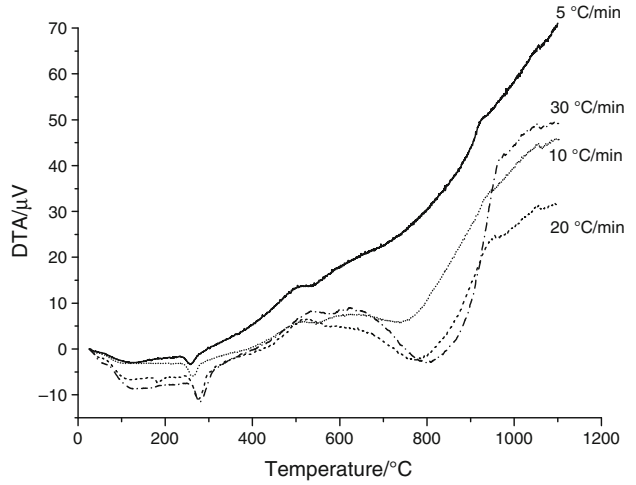

Fig. 3 DTA curves of concrete samples at heating rates of 5, 10, 20, and 30 °C/min

Table 6 Peak temperatures and heat amounts of concrete during heating at 5, 10, 20, and 30 °C/min heating rates

Heating rates/°C/min	T_1/°C	Q_1/J/g	T_2/°C	Q_2/J/g	T_3/°C	Q_3/J/g	T_4/°C	Q_4/kJ/g
5	95	−52	258	−21	568	−8	647	−0.5
10	119	−7	263	−16	545	−7	737	−0.4
20	122	−12	277	−14	542	−2	775	−0.2
30	132	−10	279	−9	571	−2	796	−0.4

Differential thermal analysis

Well-designed concrete attains strength only after hydration of cement [6]. Due to a poor crystallinity of the hydration products formed at early age hydration and low water to cement ratio, the differential thermal analysis (DTA) method is a promising one regarding its qualitative and quantitative characterization [7]. Figure 3 shows the non-isothermal DTA curves of concrete samples at four different heating rates (5, 10, 20, and 30 °C/min). Thus, dehydration of cement is endothermic process which takes place in two main steps, at about 110 and 290 °C [8], as shown in Fig. 3. An endothermic hump appears at around 560 °C, which was induced by the crystallization process of amorphous TiO_2 to crystalline TiO_2 [9]. At a higher wide temperature range of 646–796 °C, a strong endothermal peak was observed which, probably, was induced by the $MgCO_3$ decomposition into MgO and CO_2. With the increasing heating rate, the endothermic peak shifted to higher temperature and the peak become stronger and more pronounced.

The peak temperatures T_p at which transformation peaks appeared at different heating rates are listed in Table 6, along with the appropriate heat amounts.

Therefore, first peak of $Ca_{12}Al_7H_8$ dehydration in Fig. 3 occurring in the temperature range from 95 to 132 °C is due to desorption of physically adsorbed and interlayer water molecules. The second broad dehydration peak in a temperature range from 258 to 280 °C is a consequence of a dehydroxylation of the lattices and decomposition of the interlayer anions. Dehydroxylation of OH bound to tetrahedral Al is claimed as the origin of a stage 200–240 °C, while the stage 240–330 °C has been attributed to dehydroxylation of OH octahedral bound to Ca and Al. It can be argued that octahedral Al–OH decomposes after the interlayer tetrahedral Al–OH due to greater compactness of octahedral layer. According to Ukrainczyk et al. [7], three interlayer water molecules are lost during first dehydration peak at about 110 °C and five molecules of water exit the structure during second dehydration peak.

One can notice that activation energy of first step is probably lower than activation energy regarding second step for the same processes of dehydration, owing to lower energy needed for dehydration from smaller capillary pores than from much larger gel pores, which is in a great accordance with the statement given previously regarding numbers of water molecules exiting the structure during heating process.

Also, these results could be associated with values of bond energies (E_b) for CH and AH compounds.[1] Having in mind that $E_b(CaH_2) = 2{,}410$ kJ/mol and $E_b(AlH_3) = 5{,}924$ kJ/mol and if our assumption that first dehydration peak is a consequence of CaH_2 decomposition and the second dehydration peak is due to AlH_3 decomposition is right, one can notice that higher energy is needed for breaking the AlH_3 bonds than breaking the CaH_2 bonds.

Summary

Dehydration is the main process which takes place during refractory concrete sintering. Dehydration kinetics of refractory concrete, synthesized by reaction between calcium aluminates cement and alumina aggregate at elevated temperature was studied by means of DTA method under non-isothermal conditions. As seen from the results of thermal analysis, dehydration of cement proceeds in two main steps, during which a loss of three (at 110 °C) and five molecules of water (at 290 °C) occurs. In those two main steps, the following processes take place: desorption of physically adsorbed and interlayer water, dehydroxylation of the lattice, and decomposition of interlayer anions.

Acknowledgements The authors would like to thank Dr. Miodrag Mitrić for the XRD measurements. This study has been supported by

[1] http://www.webelements.com/lattice_energies.html.

Serbian Ministry of Science under projects 172057 and 45008 and by the Serbian Academy of Sciences and Arts under project F7.

References

1. Lee WE, Viera W, Zhang S, et al. Castable refractory concretes. Int Mat Rev. 2001;46:145–67.
2. Compas A, Mohmel S, Gebner W, et al. The Behaviour of CA/CA2 Cements During. Hydration and Thermal Treatment. In: Proceedings of UNITECR'97, New Orleans; 1997. p. 1273–82.
3. Terzic A, Pavlovic Lj. Application of results of non-destructive testing methods in investigation of microstructure of refractory concrete. J Mater Civ Eng. 2010;22:853–8.
4. Tongsheng Z, Qijun Y, Jiangxiong W, Peng G, Pingping Z. Study on optimization of hydration process of blended cement. J Therm Anal Calorim. doi:10.1007/s10973-011-1531-8.
5. Brown PW, Shi D, Skalny JP. Porosity/permeability relationships concrete microstructure porosity and permeability. Washington, DC: Strategic Highway Research Program, NRC; 1993. p. 43–75.
6. Vedalakshmi R, Sundara Raj A, Srinivasan S, Ganesh Babu K. Quantification of hydrated cement products of blended cements in low and medium strength concrete using TG and DTA technique. Thermochim Acta. 2003;407:49–60.
7. Ukrainczyk N, Matusinovic T, Kurajica S, Zimmermann B, Sipusic J. Dehydration of a layered double hydroxide-C_2AH_8. Thermochim Acta. 2007;464:7–15.
8. Pacewska B, Nowacka M, Wilinska I, Kubissa W, Antonovich V. Studies on the influence of spent FCC catalyst on hydration of calcium aluminate cements at ambient temperature. J Therm Anal Calorim. 2011;105:129–40.
9. Li D, Chen S, Wang D, et al. Thermo-analysis of nanocrystalline TiO_2 ceramics during the whole sintering process using differential scanning calorimetry. Ceram Int. 2010;36:827–9.